Journal of Magnetics 12(4), 156-160 (2007)

Optical Current Measuring System for Compensating Interference by Adjacent Electric Wires

Jae Kyong Cho*

Department of Electrical and Electronic Engineering, Engineering Research Institute, Gyeongsang National University, 900 Gazwa, Jinju, Gyeongnam 600-701, Korea

(Received 6 September 2007)

In this paper, we analyze the errors associated with magnetic field interference for fiber-optic current sensors working in a three-phase electric system and provide a solution to compensate the interference. For many practical conductor arrangements, the magnetic filed interference may cause errors unacceptable for the accuracy requirements of the sensors. We devised a real time compensation method for the interference by introducing geometric and weight factors. We realized the method using simple electronic circuits and obtained the real time compensated outputs with errors of ±1%.

Keywords : fiber-optic current sensor, optical current sensor, Faraday cell, current measurement, magnetic field interference

1. Introduction

Optical current sensing techniques have been internationally researched over the past 30 years. Such sensors offer a range of potential improvements such as reduced insulation requirements, increased operational bandwidth, weight and space minimization, and safe failure modes [1-3]. We describe in this paper the operation of optical current sensors using Faraday cell within environments that will be encountered in field applications. In these environments the wires carrying large currents are often placed closely to save space so that the magnetic field interference from adjacent cables made measurement error large [4]. This paper evaluates the magnitude of the interference and proposes a means whereby the interference can be reduced.

1.1. Principle of operation of optical current sensor

Figure 1 shows the schematic structure of an optical current sensor or an magneto-optic Faraday cell current sensor used in this research [2, 4, 5]. The sensor was composed of a light emitting diode (LED) as a light source, optical fibers to transmit the light, rod lenses to collimate and condense the light, polarizing beam splitters (PBSs) as a polarizer and an analyzer, a garnet Faraday cell [2, 4] to modulate the light according to the applied magnetic field, a photodiode to convert the light signal to electric signal, and an electronic circuit to drive the LED and to

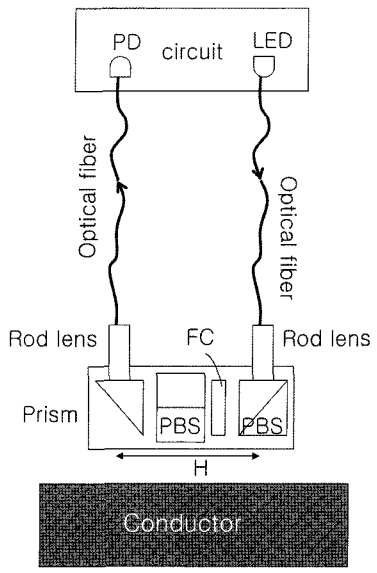

Fig. 1. Schematic structure of optical current sensor used in this research. LED: Light Emitting Diode, PD: Photo-Diode, PBS: Polarizing Beam Splitter, FC: Faraday Cell, H: Magnetic Field. The analyzing PBS was installed to be rotated by an angle of 45 degree to apply an optical bias.

*Corresponding author: Tel: +82-55-751-5364,
Fax: +82-55-762-2952, e-mail: jkcho@gnu.ac.kr

process the signal obtained by the photodiode.

The light from the source was transmitted through the optical fiber, collimated by the rod lens, and linearly polarized by the PBS. When the linearly polarized light passes through the Faraday cell under a magnetic field induced by the AC current of the conductor, the plane of the polarization rotates proportional to the magnitude of the magnetic field. The rotation angle θ_F of the plane of the polarization is described as

$$\theta_F = VHL \cos\theta \quad (1)$$

where V is Verdet constant, H is intensity of magnetic field. L is the thickness of the Faraday cell, and θ is the angle between the direction of the light propagation and the magnetic field.

The rotated linearly polarized light by the Faraday cell is changed into light intensity by the analyzer or the PBS. The analyzing PBS was installed to be rotated by an angle of 45 degree to apply an optical bias. The light, then, is reflected by the prism, condensed by the rod lens, transmitted through the optical fiber, and reaches the photodiode. The photodiode transforms the optical signal to an electric signal and the circuit processes the signal and produces the output signal proportional to the intensity of the magnetic field or the current.

1.2. Magnetic field interference

Consider a system in which three conductors carrying three-phase current are separated on a plane and the optical current sensors are attached on top of the conductors, respectively. Label the conductors as conductors 1, 2, and 3 and the sensors as S_1, S_2 and S_3.

Let the three-phase current of the conductors 1, 2, 3 be I_1, I_2, I_3 and the output signals of the sensors S_1, S_2, S_3 be V_1^S, V_2^S, V_3^S respectively, then they can be related as shown in equation (2).

$$g_{11}I_1 + g_{12}I_2 + g_{13}I_3 = V_1^S \quad (2a)$$

$$g_{21}I_1 + g_{22}I_2 + g_{23}I_3 = V_2^S \quad (2b)$$

$$g_{31}I_1 + g_{32}I_2 + g_{33}I_3 = V_3^S \quad (2c) \quad (2)$$

In equation (2) g_{11}, g_{12}, g_{13}, g_{21}, g_{22}, g_{23}, g_{31}, g_{32}, g_{33} are geometric factors affected by the geometry and configuration of the sensors and conductors. The first term $g_{11}I_1$ in equation (2a) represents the magnetic filed from the conductor 1 with current I_1. The second term $g_{12}I_2$ in equation (2a) shows the magnetic field from the conductor 2 with current I_2. The third term $g_{13}I_3$ in equation (2a) denotes the magnetic field from conductor 3 with current I_3.

The first term in equation (2a) is proportional to the current I_1 of the conductor 1 that we want to measure. The second and the third terms in equation (2a) play a role of interference because they come from conductors 2 and 3.

The sensor S_1 picks up all magnetic fields represented by the first, second and third terms in equation (2a) and gives output signal V_1^S. Let us call this 'raw signal' to differentiate from the compensated output discussed later.

Similarly the first and third terms in equation (2b) are the interfering terms when we try to measure the current I_2 of the conductor 2. For the current I_3 of the conductor 3 the first and second terms are the interfering terms.

Therefore unless the conductors placed far enough so that the interfering terms can be ignored, the interference can not be avoid.

To measure the magnetic interference we built an experimental set up as shown in Figure 2. The set up was composed of three conductors, current sources, and sensors installed on top of the conductors. Alternating currents have been applied to the conductors using the current sources. The phases of the currents were different from each other as 120 degree. The raw signals (V_1^S, V_2^S and V_3^S) of the sensors were monitored by the oscilloscope A. The current applied were monitored using standard CTs (Current Transducers, not shown in the figure) at the position where the conductors were separated far enough so that the interfering magnetic field of the adjacent conductors could be ignored.

Table 1 shows the errors (e_1^S, e_2^S and e_3^S) of the raw signals (V_1^S, V_2^S and V_3^S) of the sensors when $I_1 = I_2 = I_3 =$ 1000 A. As shown in the table the errors were unacceptably large before being compensated due to the magnetic field interference from the adjacent conductors.

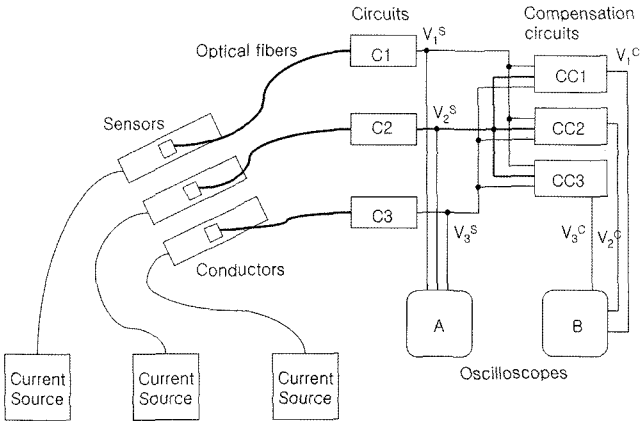

Fig. 2. Schematic diagram of experiment set up to measure the magnetic field interference. Also shown are the compensation circuits CC_1, CC_2, CC_3 to reduce the interferenece.

Table 1. The errors e_1^S, e_2^S and e_3^S of raw signals V_1^S, V_2^S and V_3^S of the sensors S_1, S_2 and S_3 experimentally obtained, when $I_1 = I_2 = I_3 = 1000$ A.

I_1 (A)	I_2 (A)	I_3 (A)	e_1^S (%)	e_2^S (%)	e_3^S (%)
1000	1000	1000	–16	–25	–8

1.3. Interference compensation

To compensate the interference we need to know the geometric factors in equation (2). They were determined experimentally as follows.

First, we applied 1000 A (I_1) to conductor 1 and zero current to conductors 2 and 3 ($I_2 = I_3 = 0$). We read the raw signals V_1^S, V_2^S and V_3^S of the sensors. We substituted the known values of I_1, $I_2 = I_3 = 0$, V_1^S, V_2^S and V_3^S into simultaneous equations (2) and calculated g_{11}, g_{21} and g_{31}.

Second, we applied 1000 A (I_2) to conductor 2, and zero current to conductors 1 and 3 ($I_1 = I_3 = 0$). We read the raw signals V_1^S, V_2^S and V_3^S of the sensors. We substituted the known values of I_2, $I_1 = I_3 = 0$, V_1^S, V_2^S and V_3^S into simultaneous equations (2) and calculated g_{12}, g_{22} and g_{32}.

Third, we applied 1000 A (I_3) to conductor 3, and zero current to conductors 1 and 2 ($I_1 = I_2 = 0$). We read the raw signals V_1^S, V_2^S and V_3^S of the sensors. We substituted the known values of I_3, $I_1 = I_2 = 0$, V_1^S, V_2^S and V_3^S into simultaneous equations (2) and calculated g_{13}, g_{23} and g_{33}.

Table 2 shows the raw signals V_1^S, V_2^S and V_3^S of the sensors so obtained. The geometric factors so obtained are shown in equation (3).

$$\begin{bmatrix} g_{11} & g_{12} & g_{13} \\ g_{21} & g_{22} & g_{23} \\ g_{31} & g_{32} & g_{33} \end{bmatrix} = \begin{bmatrix} 0.6 & 0.07 & 0.025 \\ 0.067 & 0.6 & 0.084 \\ 0.016 & 0.031 & 0.6 \end{bmatrix} \quad (3)$$

Because the conductors and the sensors of the set up were placed in a plane and separated similarly, the diagonal elements g_{11}, g_{22} and g_{33} of the geometric factor matrix were equal, the off-diagonal elements g_{12}, g_{21}, g_{23} and g_{32} were similar, and g_{13} and g_{31} were similar. If the conductors and the sensors were placed with an equal distance, the matrix would be symmetric.

Table 2. The raw signals V_1^S, V_2^S and V_3^S of the sensors S_1, S_2 and S_3 experimentally obtained to determine the geometric factors.

I_1 (A)	I_2 (A)	I_3 (A)	V_1^S (mV)	V_2^S (mV)	V_3^S (mV)
1000	0	0	600	67	16
0	1000	0	70	600	31
0	0	1000	25	84	600

Because what we want to know are the currents I_1, I_2 and I_3 of conductors 1, 2, and 3, we need to substitute the geometric factors obtained into the simultaneous equations (2) and solve them about I_1, I_2 and I_3, which will give us simultaneous equations of the form of equation (4).

$$I_1 = \alpha_{11}V_1^S + \alpha_{12}V_2^S + \alpha_{13}V_3^S = V_1^C \quad (4a)$$

$$I_2 = \alpha_{21}V_1^S + \alpha_{22}V_2^S + \alpha_{23}V_3^S = V_2^C \quad (4b)$$

$$I_3 = \alpha_{31}V_1^S + \alpha_{32}V_2^S + \alpha_{33}V_3^S = V_3^C \quad (4c) \quad (4)$$

The coefficients α_{11}, α_{12}, α_{13}, α_{21}, α_{22}, α_{23}, α_{31}, α_{32}, α_{33} are weight factors and V_1^C, V_2^C, V_3^C are the compensated outputs for conductor 1, 2, 3. Note that the compensated outputs V_1^C, V_2^C, V_3^C are expressed by the raw signals V_1^S, V_2^S and V_3^S of the sensors.

Equation (5) shows the weight factors calculated by substituting the geometric factors into equation (2) and solving the equation about I_1, I_2 and I_3.

$$\begin{bmatrix} \alpha_{11} & \alpha_{12} & \alpha_{13} \\ \alpha_{21} & \alpha_{22} & \alpha_{23} \\ \alpha_{31} & \alpha_{32} & \alpha_{33} \end{bmatrix} = \begin{bmatrix} 1.689 & -0.195 & -0.043 \\ -0.184 & 1.700 & -0.230 \\ -0.036 & -0.083 & 1.680 \end{bmatrix} \quad (5)$$

Note that the signs of the diagonal elements α_{11}, α_{22}, and α_{33} of the weight factor matrix were positive and those of rest of the weight factors were negative reflecting the compensation nature. Because the conductors and the sensors of the set up were placed in a plane and separated similarly, α_{11}, α_{22}, and α_{33} were similar, α_{12}, α_{21}, and α_{23} and α_{32} were similar, and α_{13} and α_{31} were similar.

To obtain the compensated outputs we built three compensation circuits (CC_1, CC_2, CC_3) as shown in Figure 2. Each compensation circuit gathered three raw signals V_1^S, V_2^S and V_3^S from three sensors, compensated the magnetic field interference from adjacent conductors by performing calculations based on equation (4), and produced the compensated output proportional to the current of the conductor to be measured.

Figure 3 shows a circuit diagram of one (CC_1) of the compensation circuits used to obtain the compensated output V_1^C for the current of conductor 1. The circuit was mainly composed of op amps and variable resistors. In the figure, V_1^S, V_2^S, V_3^S were the raw signals obtained from the sensor S_1, S_2, S_3, respectively. By adjusting the variable resistors VR_1, VR_2, VR_3, the weight factors, α_{11}, α_{12}, α_{13} in equation (4a) have been set. Then the weighted signals have been added using op amps OP_4, OP_5. The final variable resistor VR_4 and op amp OP_6 were used to adjust the magnitude of the compensated output signal.

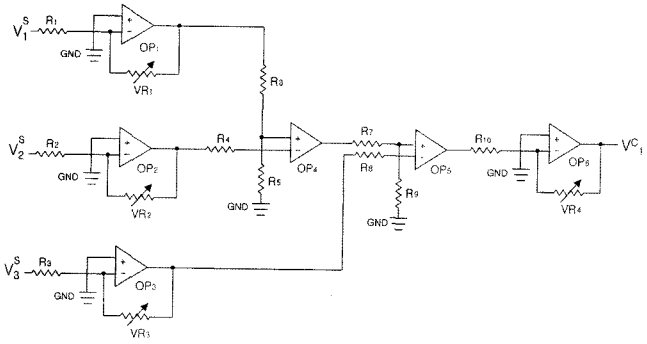

Fig. 3. Circuit diagram of a compensation circuit (CC_1). The V_1^S, V_2^S and V_3^S denote the raw signals from the sensors S_1, S_2 and S_3. The *R*, *VR* and *OP* represent resistor, variable resistor, and op amp. The *GND* denotes ground.

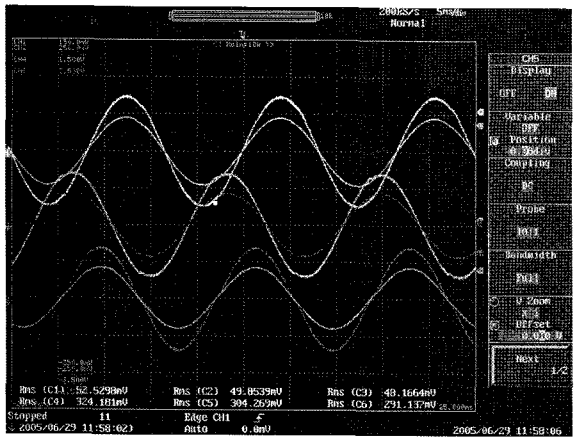

Fig. 4. The compensated output curves monitored by the oscilloscope B (See Figure 2) when $I_1 = I_2 = I_3 = 500$ A.

The compensation circuits CC_2 and CC_3 were composed and operated similarly to the compensated circuit CC_1.

Now we applied alternating currents to the conductors and monitored the compensated outputs V_1^C, V_2^C and V_3^C using the oscilloscope B in Figure 2. The currents were varied in the range from 500 A to 2500 A, maintaining $I_1 = I_2 = I_3$.

Figure 4 shows the compensated output curves monitored by the oscilloscope B when $I_1 = I_2 = I_3 = 500$ A. Three curves having lager amplitudes were the compensated output curves. Three curves having smaller amplitudes were the corresponding output curves of the standard CTs. Note that the compensated output curves closely resemble those of the standard CTs in amplitude ratio and phase. Other curves for different current values were similar to Figure 4.

Figure 5(a), (b) and (c) show the compensated outputs V_1^C, V_2^C and V_3^C, respectively, as a function of applied current ($I_1 = I_2 = I_3$). As shown in the figure a good linearity has been obtained for all three compensated outputs.

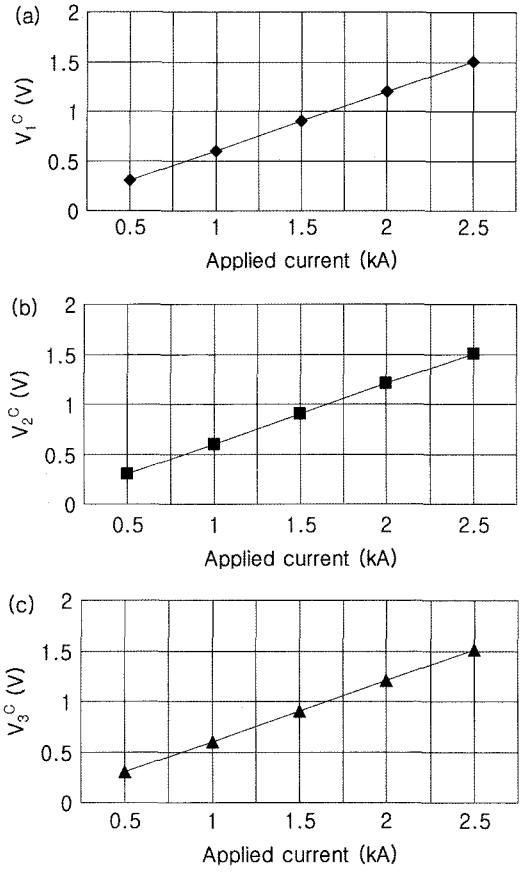

Fig. 5. The compensated outputs (a) V_1^C, (b) V_2^C and (c) V_3^C, respectively, as a function of applied current ($I_1 = I_2 = I_3$).

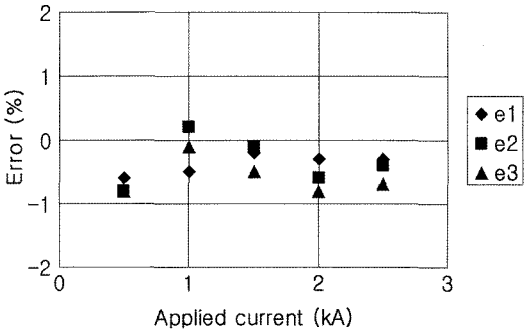

Fig. 6. Errors e_1, e_2, e_3 for the compensated outputs V_1^C, V_2^C and V_3^C, respectively.

Figure 6 shows errors e_1, e_2, e_3 for the compensated outputs V_1^C, V_2^C and V_3^C. As shown in the figure the errors were within ± 1%. It is expected that this error can be reduced more if the geometric factor can be determined more precisely.

The above results show that the compensated outputs can be obtained from the linear combination of the raw signals of the sensors. The compensation method discussed here can be applied to other current transducers. They can be fiber optic current transducers utilizing magneto-

strictive elements or interferometers. They need not to be optical transducers. They can be electromagnetic current transducers that pick up magnetic fields to sense the current.

The compensated method discussed here can be generalized for the system having more and less conductors. The generalization is straight forward. As the number of conductors increases or decreases, the number of equations accordingly increases or decreases.

2. Conclusions

We analyzed the errors associated with magnetic field interference for fiber-optic current sensors working in a three-phase electric system. For the conductor arrangement investigated that resembled practical electric system, the magnetic field interference caused errors unacceptable for the accuracy requirements of the sensors. We devised a real time compensation method to reduce the interference by introducing geometric and weight factors. We realized the method using simple electronic circuits and obtained the real time compensated outputs with errors of ± 1%.

Acknowledgement

This work was supported by the fund of Research Promotion Program (RPP-2007-000), Gyeongsang National University.

References

[1] K. Kyuma and M. Hushita, Optical fiber sensor (In Japanese), Johozoshakai, Tokyo, pp. 110-117 (1987).
[2] N. Itoh, H. Minemoto, D. Ishiko, and S. Ishizuka, IEEE Transaction on Magnetics **31**, 3191 (1995).
[3] T. Fujimoto, M. Shinrizu, H. Nakagawa, I. Sone, K. KawashimaI, and E. Mori, IEEE Transactions on Power Delivery **12**, 45 (1997).
[4] O. Kamada, H. Minemoto, and S. Ishizuka, J. Appl. Phys. **61**, 3268 (1987).
[5] P. I. Nkitin, A. N. Grigorenko, and A. I. Savchuk, Sensors and Materials **4**, 205 (1993).
[6] S. Kajiwara, Y. Watanabe, and T. Tanimizu, Hitachi Review **49**, 93 (2000).